Essential amino acid transporter Lat4 (Slc43a2) is required for mouse development

Guetg, Adriano ; Mariotta, Luca ; Bock, Lukas ; Herzog, Brigitte ; Fingerhut, Ralph ; Camargo, Simone M R ; Verrey, François

Abstract: KEY POINTS: Lat4 (Slc43a2) transports branched-chain amino acids, phenylalanine and methionine, and is expressed in kidney tubule and small intestine epithelial cells. Using a new knockout model as a negative control, it is shown that Lat4 is expressed at the basolateral side of small intestine enterocytes and kidney epithelial cells of the proximal tubule, thick ascending limb and distal convoluted tubule. In the Xenopus oocyte expression system, Lat4 is shown to function as a uniporter with symmetric intracellular and extracellular apparent affinities for phenylalanine. Mice lacking Lat4 display a slight intrauterine growth restriction, postnatal malnutrition and early death, presumably as a result of defective amino acid (re)absorption. These results demonstrate the crucial role that the uniporter Lat4 plays for amino acid transport across cellular barriers and mouse development. ABSTRACT: Amino acid (AA) uniporter Lat4 (Slc43a2) mediates facilitated diffusion of branched-chain AAs, methionine and phenylalanine, although its physiological role and subcellular localization are not known. We report that Slc43a2 knockout mice were born at expected Mendelian frequency but displayed an ~10% intrauterine growth retardation and low amniotic fluid AAs, suggesting defective transplacental transport. Postnatal growth was strongly reduced, with premature death occurring within 9 days such that further investigations were made within 3 days of birth. Lat4 immunofluorescence showed a strong basolateral signal in the small intestine, kidney proximal tubule and thick ascending limb epithelial cells of wild-type but not Slc43a2 null littermates and no signal in liver and skeletal muscle. Experiments using Xenopus laevis oocytes demonstrated that Lat4 functioned as a symmetrical low affinity uniporter with a K0.5 of ~5 mm for both in- and efflux. Plasma AA concentration was decreased in Slc43a2 null pups, in particular that of non-essential AAs alanine, serine, histidine and proline. Together with an increased level of plasma long chain acylcarnitines and a strong alteration of liver gene expression, this indicates malnutrition. Attempts to rescue pups by decreasing the litter size or by nutrients injected i.p. did not succeed. Radioactively labelled leucine but not lysine given per os accumulated in the small intestine of Slc43a2null pups, suggesting the defective transcellular transport of Lat4 substrates. In summary, Lat4 is a symmetrical uniporter for neutral essential AAs localizing at the basolateral side of (re)absorbing epithelia and is necessary for early nutrition and development.

DOI: https://doi.org/10.1113/jphysiol.2014.283960

DOI: https://doi.org/10.1113/jphysiol.2014.283960

Title: Essential amino acid transporter Lat4 (*Slc43a2*) is required for mouse development

Authors: Adriano Guetg[1], Luca Mariotta[1], Lukas Bock[1], Brigitte Herzog[1], Ralph Fingerhut[2], Simone M.R. Camargo[1] and François Verrey[1].

Affiliation: [1]Institute of Physiology and Zurich Center of Integrative Human Physiology, University of Zurich, Switzerland. [2]University Children's Hospital, Children`s Research Center, Zurich, Switzerland

Additional information:

A) Running title: Lat4 (*Slc43a2*) is required for mice development

B) Keywords: Lat4 (*Slc43a2*), system L amino acid transporter, branched-chain amino acids, placenta, growth, malnutrition

C) Total words in the paper excluding figure legends and references: 7432

D) Corresponding Author: François Verrey

Institute of Physiology, University of Zürich

Winterthurerstr. 190, CH-8057 Zürich, Switzerland

Phone +41 44 635 50 44/46 Fax +41 635 68 14

verrey@access.uzh.ch

Key points summary:

- Lat4 (*Slc43a2*) transports branched-chain amino acids, phenylalanine and methionine and is expressed in kidney tubule and small intestine epithelial cells.
- Using a new knock out model as negative control, it is shown that Lat4 is expressed at the basolateral side of small intestine enterocytes and kidney epithelial cells of the proximal tubule, thick ascending limb and distal convoluted tubule.
- In the *Xenopus* oocytes expression system Lat4 is shown to function as a uniporter with symmetric intracellular and extracellular apparent affinities for phenylalanine.
- Mice lacking Lat4 display a slight intrauterine growth restriction, postnatal malnutrition and early death, presumably due to defective amino acid (re)absorption.
- These results demonstrate the crucial role that the uniporter LAT4 plays for amino acids transport across cellular barriers and mouse development.

124 words

Abstract

Amino acid uniporter Lat4 (*Slc43a2*) mediates facilitated diffusion of branched-chain amino acids, methionine and phenylalanine, but its physiological role and subcellular localization are not known. We report here that *Slc43a2* knock-out mice were born at expected Mendelian frequency but displayed an ~10% intrauterine growth retardation and low amniotic fluid amino acids suggesting defective transplacental transport. Postnatal growth was strongly reduced with premature death occurring within 9 days such that further investigations were made within three days after birth. Lat4 immunofluorescence showed a strong basolateral signal in small intestine, kidney proximal tubule and thick ascending limb epithelial cells of wild type but not *Slc43a2*-null littermates and no signal in liver and skeletal muscle. Experiments in *Xenopus laevis* oocytes demonstrated that Lat4 functions as symmetrical low affinity uniporter with a $K_{0.5}$ of ~5 mM for both in- and efflux. Plasma amino acid concentration was decreased in *Slc43a2*-null pups, in particular that of non-essential amino acids alanine, serine, histidine and proline. Together with an increased level of plasma long chain acylcarnitines and a strong alteration of liver gene expression, this indicates malnutrition. Attempts to rescue pups by decreasing the litter size or by intraperitoneal nutrients injection didn't succeed. Radioactively labeled leucine but not lysine given *per os* accumulated in small intestine of *Slc43a2* null pups suggesting defective transcellular transport of Lat4 substrates. Taken together, Lat4 is a symmetrical uniporter for neutral essential amino acids localizing at the basolateral side of (re)absorbing epithelia and is necessary for early nutrition and development.

Abbreviations: AA, amino acid; DA, dicarboxylacylcarnitine; DCT, distal convoluted tubule; LPI, lysinuric protein intolerance; NCC, sodium-chloride cotransporter; NKCC2, sodium-potassium-chloride cotransporter 2; PT, proximal tubule; TAL, thick ascending limb.

Introduction

Dietary protein intake is an essential and tightly regulated process, which needs to meet the physiological body requirements especially during highly anabolic periods (Poncet & Taylor, 2013). The enzyme-mediated hydrolysis of dietary proteins in the gastrointestinal lumen produces oligopeptides and individual amino acids (AAs) that are absorbed by moving sequentially across apical and basolateral cell membranes of small intestine enterocytes (Nassl *et al.*, 2011). The zwitterionic nature of neutral AAs prevents direct crossing of the epithelial lipid bilayer by simple diffusion and imposes the presence of membrane-spanning transporter proteins (Braun *et al.*, 2011). Severe malabsorption and aminoaciduria syndromes have been linked to defects of specific AA transporters substantiating the essential role, which transepithelial transport plays for body AA homeostasis (Verrey *et al.*, 2009; Broer & Palacin, 2011).

The luminal step of neutral AA absorption and reabsorption at the level of the small intestine and kidney, respectively, is to a large extent mediated by the apical transporter B^0AT1 (*SLC6A19*). This luminal symporter uses the driving force exerted by the Na^+ gradient and the membrane potential on the co-transported Na^+ ion for the concentrative import of its neutral amino acid substrates (secondary active transport) (Rudnick et al., 2014).Once inside enterocytes or kidney proximal tubule cells, neutral AAs can be effluxed across the basolateral membrane by cooperating AA exchangers and uniporters. Indeed, all neutral AAs can be effluxed by the major basolateral neutral AA antiporter (obligatory exchanger) LAT2-4F2hc (*SLC7A8-SLC3A2*). It is however important to realize that for each exported AA this antiporter imports another AA. Thus, this antiporter does not perform a net transmembrane AA efflux (Meier *et al.*, 2002). Surprisingly, no genetic diseases involving defects of LAT2-4F2hc have been described yet, whereas mutations in the other basolateral antiporter y^+LAT1-4F2hc (*SLC7A7-SLC3A2*), which exchanges preferentially intracellular cationic AAs against neutral AAs and $Na^{+,}$ cause the autosomal recessive disease lysinuric protein intolerance (LPI) (Borsani *et al.*, 1999). The respective physiological roles of both exchangers were also investigated using knock-out (KO) mice. While the lack of LAT2 resulted in a mild phenotype with a minor aminoaciduria (Braun *et al.*, 2011), the lack of y^+LAT1 caused intrauterine growth restriction and resulted in premature death for about 90% of the newborn *Slc7a7*$^{-/-}$ homozygous mice (Sperandeo *et al.*, 2007).

To achieve a net efflux of all different AAs from small intestine enterocytes and proximal kidney tubule epithelial cells, transporters are required that mediate the net efflux of some AAs that can then recycle into the cells via the above mentioned antiporters and thereby drive their efflux activity (Verrey *et al.*, 2009). The T-type aromatic AA uniporter TAT1 (SLC16A10*)* represents the best

characterized such transporter expressed at the basolateral membrane (Ramadan *et al.*, 2006; Ramadan *et al.*, 2007). Using the *Xenopus laevis* oocytes expression system it has indeed been shown to mediate the facilitated diffusion of the essential aromatic AAs phenylalanine, tryptophan and tyrosine with symmetric apparent affinities (i.e. $K_m \approx 30$ mM for phenylalanine) and thereby drive the efflux of other LAT2-4F2hc substrates such as the non-essential AA glutamine (Ramadan *et al.*, 2006; Ramadan *et al.*, 2007). Recently, we characterized the physiological role of TAT1 using *Slc16a10* deficient mice. Interestingly, these mice presented a mild phenotype with increased plasma, kidney and muscle aromatic AAs, independently of dietary protein quantity, combined with a major aromatic aminoaciduria under high protein diet (Mariotta *et al.*, 2012). The lack of neurological symptoms and important metabolic dysfunctions despite the defective intestinal absorption of aromatic AAs like phenylalanine, which is the metabolic precursors of the hormone thyroxin and the neurotransmitter dopamine, suggested a possible compensatory mechanism by (an)other basolateral uniporter(s). We suggested that the uniporter LAT4 (*SLC43A2*) could play this role.

LAT4 belongs to the SLC43 family which includes two additional members: LAT3 (SLC43A1), which is a uniporter for large essential neutral AAs and has been shown to be upregulated in liver and skeletal muscle upon starvation and displays only a low mRNA expression level in small intestine and kidney (Babu et al., 2003; Fukuhara et al., 2007), and EEG1 (SLC43A3), the function of which is still unknown. The latter gene product has been recently shown by Bodoy et al. to be prominently expressed in human liver and heart and, based on immunohistochemistry, to be expressed at the basolateral membrane of human kidney proximal convoluted tubule (Bodoy et al., 2005). LAT4 shows only about 30% identity with EEG1 and has been shown by Northern blot analysis of human RNA to be highly expressed in placenta, peripheral blood leucocytes and kidney and additionally, by Northern blot analysis of mouse RNA, to be expressed in small intestine and brain (Bodoy et al., 2005). Microarray data available on internet (BioGPS.org) confirm these localizations and additionally show substantial expression in macrophages, microglia and osteoclasts. Based on *in situ* hybridization, Lat4 was suggested to be expressed in kidney distal tubule and collecting duct and the images appeared also compatible with expression in proximal tubule. In small intestine, the signal localized more to crypt cells (Bodoy et al., 2005). Lat4 mRNA was also detected in cell lines isolated from mouse kidney proximal tubule, in agreement with the mRNA expression in isolated proximal tubules reported by Cheval et al. (Cheval et al., 2011). Furthermore, kinetic analysis of phenylalanine uptake in these cells suggested Lat4 involvement, supporting the possibility that this uniporter might play a role in proximal tubule AA reabsorption.

The preferential substrates of LAT4 are only essential AAs, specifically the branched-chain ones (leucine, isoleucine, valine) and additionally phenylalanine and methionine (Bodoy *et al.*, 2005; Wu, 2009). To test the physiological role of Lat4 in whole-body AA homeostasis and epithelial transport, we generated a global *Slc43a2* $^{-/-}$ KO mouse and provide in the following report the analysis of its phenotype.

Materials and Methods

Ethical approval. All procedures for mice handling and experimental interventions were according to the Swiss Animal Welfare laws and approved by the Kantonales Veterinäramt Zürich.

Generation of *Slc43a2/Lat4*$^{-/-}$ *KO* mice by gene trapping. The *Slc43a2*$^{-/-}$ KO mouse was produced by the Phenogenomic Center of Toronto (www.phenogenomics.ca). Embryonic stem (ES) cell lines were mutated by insertional mutagenesis using a UPA gene trap vector (Shigeoka *et al.*, 2005) in the 6th intron of the *Slc43a2* gene. Cells were prepared for aggregation with diploid embryos to produce chimeric mice. R1 cells were in a 129 mouse background, whereas the germline was tested by crossing the chimera to CD-1 mice and assessing coat color. The interruption of the gene leads to the production of a truncated transcript presumably subject to nonsense mediated decay and thus of low abundance. Mice were bred into C57BL/6 background. All animals were housed in standard conditions and fed a standard diet prior experiment.

Antibodies. Anti-mouse Lat4 antibodies targeted to the C-terminal peptide (N-CQLQQKREDSKLFL-C) were raised in rabbit; whereas anti-mouse Tmem27 antibodies targeted to the C-terminal peptide (N-CDPLDMKGGHINDGFLT-C) and anti-mouse B^0AT1 antibodies targeted to the N-terminal peptide (N-MVRLVLPNPGLEERIC-C) were raised in guinea-pig (Pineda, Berlin, Germany). Anti-mouse NCC (Loffing *et al.*, 2004), anti-mouse NKCC2 (Kaplan *et al.*, 1996), anti-mouse MDR1 (Fickert *et al.*, 2001) were previously characterized.

Immunofluorescence. Organs were isolated and immediately frozen in liquid propane. 7 µm sections were prepared on Superfrost®Plus Menzel slides (Gerhard Menzel GmbH, Braunschweig, Germany). To test for Lat4 localization in NKCC2 expressing kidney tubule segments, 4 µm consecutive sections were prepared. Sections were then fixed with methanol at -20 °C for 90 seconds, rehydrated for 15 min at room-temperature (RT), washed three times for 5 min with phosphate- buffered solution (PBS) at RT. For Lat4, NCC, MDR1 and Tmem27 detection, epitope retrieval was performed by incubating slides in 10 mM sodium citrate pH 6.0 for 10 min at 98 °C with a microwave (Histos 3, Milestone, USA). For NKCC2 and Tat1 detection, no epitope retrieval was performed. Sections were then washed again three times for 5 min with PBS at RT and

incubated with blocking solution (2% bovine serum albumin, 0.04% Triton X-100 in PBS pH 7.4) for 1 hour at RT. Primary antibodies were diluted in blocking solution and incubated overnight at 4°C with the respective dilutions: 1:500 for Lat4, 1:1000 for Tmem27, 1:2000 for NKCC2, 1:500 for NCC, 1:500 for Tat1 and 1:300 for MDR1. Sections were then washed three times for 5 min in PBS at RT. The following secondary antibodies were applied with 1:500 dilutions for 1 hour at RT: Alexa Fluor® 488 anti-rabbit, Alexa Fluor® 594 anti-rabbit and Alexa Fluor® 568 anti-guinea-pig. Staining of nuclei was performed with 4',6-diamidino-2-phenylindole (DAPI) at 1:500 dilution.

Western blotting on oocyte total membrane lysates. Total membrane lysates of oocytes and western blotting were performed as described elsewhere (Ramadan *et al*., 2007).

Morphological analysis of organs. Organs isolation, 7 µm sections preparation and section fixation were performed as described before. Classical Hematoxylin & Eosin staining was performed as described elsewhere (Mariotta *et al.*, 2012).

Cloning of hLAT4 cDNA and cRNA synthesis. Human LAT4 cDNA in pTLN vector was kindly provided by Manuel Palacin (Bodoy *et al.*, 2005). The construct was linearized using the *BglII* restriction site and cRNA was synthesized using the MEGAscript high-yield *in vitro* transcription kit (Ambion, Austin, TX) according to manufacturer's instructions.

***Xenopus laevis* oocytes preparation and cRNA injection.** Oocytes at stage IV as described in (Dumont, 1972) were treated with collagenase A for 2-3 h at room temperature in Ca^{2+}-free buffer (82.5 mM NaCl, 2 mM MgCl2 and 10 mM HEPES pH 7.4) and kept at 16°C in Modified Barth's solution (88 mM NaCl, 1 mM KCl, 0.82 mM $MgSO_4$, 0.41 mM $CaCl_2$, 0.33 mM $Ca(NO_3)_2$, 2.4 mM $NaHCO_3$, 10 mM HEPES, 5 mg/l Gentamicin, 5 mg/l Doxycycline). Remaining follicular layers were manually removed. 25 ng of LAT4 cRNA was injected and oocytes were incubated for 3 days at 16°C in ND96 solution (96 mM NaCl, 2 mM KCl, 1 mM $MgCl_2$, 1.8 mM $CaCl_2$, 5 mM HEPES-Tris pH 7.4, supplemented with 50 mg/l tetracycline).

Uptake of amino acids in *Xenopus laevis* oocytes. Oocytes were washed six times with 2 ml Na^+-buffer (100 mM NaCl, 2 mM KCl, 1 mM CaCl2, 1 mM MgCl2, 10 mM HEPES pH 7.4) and then pre-warmed for 2 minutes at 25°C in a water bath. Subsequently, the pre-warming solution was aspirated and 100 µl of Na^+-buffer containing unlabeled phenylalanine at the indicated concentrations together with [^{3}H]-L-phenylalanine (10 µCi/ml) as tracer (Hartmann Analytic, Braunschweig, Germany) were added. Oocytes were then incubated for 10 minutes at 25°C. Thereafter, uptake solution was removed, oocytes were washed six times with 2 ml ice-cold Na^+-buffer and separately dissolved in 250 µl 2% SDS under agitation for at least 30 min. Upon addition of 3 ml scintillation fluid (Emulsifier-Safe™), radioactivity was counted on a liquid scintillation counter (TRI-CARB 2900TR, Packard Instrument, Meriden, CT). Uptake values were corrected by

subtracting the values obtained from non-injected oocytes. Curves corresponding to the Michaelis-Menten equation were fitted to the data sets using GraphPad Prism 5.0 (GraphPad Software, San Diego, CA).

Efflux of amino acids in *Xenopus laevis* oocytes. Oocytes were injected with 50 nl of different phenylalanine solutions (10 mM, 25 mM, 50 mM, 100 mM and 200 mM) together with [^{3}H]-L-phenylalanine (0.2 µCi/µl) as tracer. Assuming an oocyte volume of about 400 µl (Taylor & Smith, 1987), the resulting oocyte internal phenylalanine concentration upon injection corresponded respectively to 1.11 mM, 2.78 mM, 5.56 mM, 11.11 mM and 22.22 mM. Oocytes were subsequently washed four times in ND96 solution and 200 µl ND96 were given to each oocyte. Efflux was allowed to take place for 10 minutes at 25°C before recovering the ND96 solution and washing the oocyte four times with ND96. For the oocytes lysis and data analysis, see "Uptake of amino acids in *Xenopus laevis* oocytes".

RNA extraction and real-time PCR. Mice at the indicated day after birth were sacrificed by decapitation and organs were immediately rinsed several times with ice-cold PBS prior to being rapidly frozen in liquid propane until further use. Total RNA was extracted and reverse transcription was performed as described elsewhere (Ramadan *et al.*, 2006). For real-time PCR, 10 ng of cDNA template were used and the reaction was set according to Applied Biosystems recommendations (TaqMan® Universal PCR master mix, Applied Biosystems). The abundance of target mRNAs was standardized relative to 18S ribosomal RNA. Primers and probes for Lat2 (*Slc7a8*), 4F2hc (*Slc3a2*), y^+Lat1 (*Slc7a7*), y^+Lat2 (*Slc7a6*), Asct2 (*Slc1a5*), Tat1 (*Slc16a10*) and B^0AT1^0 (*Slc6a19*) were previously described (Moret *et al.*, 2007; Mariotta *et al.*, 2012). For Lat4 detection, the following primers and probe were used: 5'GCTGATTGCATATGGAGCAAGTAAC 3' (for), 5'CGAAGTGAACGTCATGCACAT 3' (rev) and 5'CTCTCTGTGCTCATCTTTATCGCCTTGGC3'. For Eeg1 detection, the following primers and probe were used: 5'GCTACATCTTTGACCGCTTCAA 3' (for), 5'CGCAGGTGTAGAAAAATATGGCTAT 3' (rev) and 5'ACTACTGTGGCCCGCC 3' (probe). For Lat3 detection, the following primers and probe were used: 5'CCCTGAATGAGAATGCTTCCTT 3' (for), 5'ATGGCATTGGTGAGCTTTTGT 3' (rev) and 5'AGCACCAAGTTCACTAGACCACGCTACCG 3' (probe).

Isolation of pups at embryonic day 18 (E18) and measurements of amino acids in amniotic fluids. Slc43a2$^{+/-}$ pregnant females were euthanized by cervical dislocation and amniotic sacs were dissected using standard laparotomy. Amniotic fluids were collected by puncturing the amniotic

sacs and amino acid measurements were performed as described previously (Mariotta *et al*. 2012). E18 pups were subsequently isolated from their amniotic sacs and weighted.

Plasma amino acid and acylcarnitine measurements. Amino acids and acylcarnitines were measured after extraction with methanol without derivatisation (Neobase Kit, Perkin Elmer, Turku, Finnland) on an Acquity-TQD tandem mass spectrometer (Waters, Milford, USA). Briefly, 3 µL of plasma were spotted onto prepunched plain filter paper (Ahlstom 226) in 96-well plain uncoated microtiter plates. Amino acids and acylcarnitines were extracted with 100 µL methanolic extraction solution containing stable isotope labelled internal standards by shaking for 45 min at 45°C. 30 µL of extract were then injected with a flow rate of 10 µL/min directly into the tandem mass spectrometer and measured afterwards in MRM-mode (multiple reaction monitoring).

RNA-Sequencing analysis of liver. Organs were isolated and RNA was extracted as described before. The quality of the isolated RNA was determined with a Qubit® (1.0) Fluorometer (Life Technologies, California, USA) and a Bioanalyzer 2100 (Agilent, Waldbronn, Germany). Only those samples with a 260 nm/280 nm ratio between 1.8–2.1 and a 28S/18S ratio within 1.5–2 were further processed. The TruSeq RNA Sample Prep Kit v2 (Illumina, Inc, California, USA) was used in the succeeding steps. Briefly, total RNA samples (100-1000 ng) were polyA enriched and then reverse-transcribed into double-stranded cDNA. The cDNA samples were fragmented, end-repaired and polyadenylated before ligation of TruSeq adapters containing the index for multiplexing. Fragments containing TruSeq adapters on both ends were selectively enriched with PCR. The quality and quantity of the enriched libraries were validated using Qubit® (1.0) Fluorometer and the Caliper GX LabChip® GX (Caliper Life Sciences, Inc., USA). The product is a smear with an average fragment size of approximately 260 bp. The libraries were normalized to 10 nM in Tris-Cl 10 mM, pH 8.5 with 0.1% Tween 20. The TruSeq PE Cluster Kit v3-cBot-HS or TruSeq SR Cluster Kit v3-cBot-HS (Illumina, Inc, California, USA) was used for cluster generation using 10 pM of pooled normalized libraries on the cBOT. Sequencing were performed on the Illumina HiSeq 2000 paired end at 2 X101 bp or single end 100 bp using the TruSeq SBS Kit v3-HS (Illumina, Inc, California, USA). RNA-seq reads were quality-checked with fastqc which computes various quality metrics for the raw reads. Reads were aligned to the genome and transcriptome with Tophat v1.3.3. Before mapping, the low quality ends of the reads were clipped (3 bases from the read start and 10 bases from the read end). Tophat v1.3.3 was run with default options. The fragment length parameter was set to 100 bases with a standard deviation of 100 bases. Based on these alignments the distribution of the reads across genomic features was assessed. Isoform expression was quantified with the RSEM algorithm (www.biomedcentral.com/1471-2105/12/323) with the option for estimation of the read start position distribution turned on. Raw data are available on the NCBI

BioProject platform (http://www.ncbi.nlm.nih.gov/bioproject/) under the BioProject ID: PRJNA226691.

Determination of radiolabeled leucine and lysine distribution after oral administration. Mice at day 2 after birth were starved for 30 min in a humidified chamber on a warming plate set at 37°C. Thereafter, 5 µl of radiolabeled amino acid solution (1 mM leucine, [^{3}H]-L-leucine 0.2 µCi/µl, 1 mM lysine, [^{14}C]-L-lysine 0.04 µCi/µl) was administered and the mouse was placed again in the aforementioned chamber for 30 min. Thereafter, mice were sacrificed by decapitation and plasma was collected as described before. Organs were isolated, rinsed several times with ice-cold PBS and weighted. Subsequently, organs were lysed in Solvable (Perkin Elmer, Switzerland) overnight at 50 °C and bleached with 200 µl of 30% H_2O_2. Radioactivity was determined upon addition of 12 ml of Ultima Gold scintillation liquid (Perkin Elmer, Switzerland) as described before. AA accumulation within each organ was normalized to organ weight.

Blood glucose measurement. Mice at day 2 were sacrificed by decapitation and blood glucose was measured with reactive test stripes Accu-Check ® (Roche Diagnostics, Mannheim, Germany).

Results

Lat4 protein absence in *Slc43a2*$^{-/-}$ mice and localization in wild type mice epithelia

The expression and localization of the Lat4 protein was investigated using a new antibody that was validated by Western blotting (Supplementary Figure 1). Immunofluorescence images of the small intestine and kidney proximal tubule of 3 days old pups confirmed the absence of Lat4 protein in *Slc43a2* null pups in comparison with wild type littermates (Fig. 1A-D). The integrity of the KO tissues showing no Lat4 signal was demonstrated by co-labeling with specific markers, for instance Tmem27 for kidney and MDR1 for liver (Fig. 1A, B, G and H). The lack of Lat4 signal in *Slc43a2* null mice additionally demonstrated the specificity of the immunofluorescence signals that localized to the basolateral membrane of kidney tubule (panel A) and small intestine (panel C) epithelial cells. As expected based on previous mRNA data (Bodoy *et al.*, 2005), Lat4 expression was not detected in skeletal muscle and liver of wild type and KO pups (Fig. 1E-H).

A strong Lat4-specific labeling was detected on small intestine villi at the basolateral membrane of enterocytes, whereas no clearly specific Lat4 signal was visible in the crypts (Fig. 2A, B). To investigate in more details the localization of Lat4 along the mouse kidney nephron, we performed co-stainings with tubule-specific markers. The strong expression of Lat4 in the proximal tubule (PT) was confirmed by labeling of the luminal SLC6-transporter accessory protein Tmem27 in the same cells (Danilczyk *et al.,* 2006) (Fig. 2C) and the colocalization with the aromatic AA uniporter Tat1 in the basolateral membrane (consecutive sections Fig. 2 D and E) (Ramadan *et al.*, 2006). A weaker expression of Lat4 was detected in the distal convoluted tubule (DCT), which was co-stained with apical sodium-chloride cotransporter (NCC) antibody (Fig 2F), whereas a strong expression of Lat4 was revealed in the thick-ascending limb of Henle's loop (TAL), which was identified by sodium-potassium-chloride cotransporter 2 (NKCC2) labeling in a consecutive section (Fig. 2G and H) (Wagner *et al.*, 2008). Taken together, our immunofluorescence data show that Lat4 protein is expressed at the basolateral membrane of small intestine enterocytes, and kidney proximal tubule, thick ascending limb and, to a minor extent, of distal convoluted tubule epithelial cells.

Kinetic properties of LAT4 expressed in *Xenopus laevis* oocytes

In the original report by Bodoy *et al.,* Lat4 was suggested to function as a uniporter based on the observation that it facilitated the efflux of phenylalanine from *Xenopus laevis* oocytes independent of extracellular AAs (Bodoy *et al.*, 2005). To determine the kinetic properties of Lat4, we performed a series of uptake and efflux rate measurements with different concentrations of

phenylalanine using the *Xenopus laevis* oocytes expression system (Fig. 3). Fitting Michaelis-Menten kinetics curves to the experimental phenylalanine uptake results, we derived a $K_{0.5}$ constant of 5.2 ± 0.5 mM (R^2 = 0.89). This value corresponds to a low-affinity transport comparable to that previously reported by Bodoy *et al.* (Bodoy *et al.*, 2005), but no additional high-affinity/low capacity component was noticed (Fig. 3A). To determine the efflux kinetic properties, oocytes were injected with increasing concentrations of phenylalanine and the resulting intracellular concentration of phenylalanine was estimated assuming an oocyte volume of 400 nl as previously described by Meier *et. al.* (Meier *et al.*, 2002). Fitting the Michaelis-Menten kinetics to the efflux values measured after 10 min yielded a low-affinity $K_{0.5}$ of 6.0 ± 1.4 mM (R^2 = 0.66), which is comparable with the apparent affinity value obtained for the uptake (Fig. 3B). Based on these results, we conclude that Lat4 shows symmetric intracellular and extracellular apparent affinities for phenylalanine.

Intrauterine growth restriction and reduced amniotic fluid amino acids concentration in *Slc43a2*$^{-/-}$ mice

Lat4 is known to be expressed in mouse placenta (Bodoy *et al*. 2005), where it might play an important role in AA transport, in particular by cooperating with the antiporter Lat2-4F2hc (Cleal *et al*. 2011). To investigate the role of Lat4 in placental AA transport and intrauterine development, we analyzed foeti isolated from *Slc43a2*$^{+/-}$ inter se crossed mice at embryonic day 18 (E18) (Fig. 4). *Slc43a2*$^{-/-}$ foeti displayed a weight reduction of about 10% compared to *Slc43a2*$^{+/+}$ and *Slc43a2*$^{+/-}$ littermates (E18 mean weight of about 0.82 g for *Slc43a2*$^{-/-}$ versus 0.93 g for *Slc43a2*$^{+/+}$) (Fig. 4B), but no additional obvious phenotypical sign (Fig. 4A). This reduced intrauterine growth did not result in prenatal lethality as the birth statistics of *Slc43a2*$^{-/-}$ mice did not differ from the expected Mendelian ratio ($p = 0.48$, χ^2-test with $n > 100$ pups). To determine the effect of Lat4 deletion on placental AA transport, we measured the AA concentration in amniotic fluid of individual pups (Fig. 4C). Interestingly, *Slc43a2*$^{-/-}$ mice displayed a marked reduction (i.e. > 50% compared to *Slc43a2*$^{+/+}$) in the concentration of almost all AAs with the exception of aspartate and glutamate that did not show a statistically significant change. Measurements of other parameters such as glucose and total protein concentration or osmolarity did not show any difference (data not shown), pointing towards a specific defect of foetal AA supply. Therefore, we conclude that the lack of Lat4 results in a defective foetal AA delivery, which is not only restricted to Lat4-specific substrates, but includes most AAs, suggesting that the defective Lat4 transport leads prenatally to a general decrease of amino acid- related transport resulting in a reduced intrauterine growth.

Growth defect, metabolic alterations and early postnatal lethality of *Slc43a2*$^{-/-}$ mice

Despite the reduced intrauterine growth reported above, *Slc43a2* $^{-/-}$ pups did not show any pathological sign at birth. They displayed a normal skin color and the presence of a white area at the left side of the abdomen, i.e. the so-called "milk spot" confirmed normal milk delivery by the mother. However, monitoring of the postnatal weight revealed that *Slc43a2*$^{-/-}$ pups gained only very little weight compared to littermates (Fig. 5A and 5B). Furthermore, they all died within few days after birth, as shown in the Kaplan-Meier survival analysis (Fig. 5C). Indeed, more than 50% of the observed *Slc43a2*$^{-/-}$ pups died until postnatal day 7 and the mortality reached 100% at day 10.

In order to obtain more information about the possible pathophysiological mechanisms underlying the early lethality, we measured the concentration of AAs in the plasma of 3 days old *Slc43a2*$^{-/-}$ pups and compared it to age-matched littermates (Fig. 6A). We observed a major decrease of certain AAs in *Slc43a2*$^{-/-}$ mice in comparison with *Slc43a2*$^{+/+}$. The highest relative difference was observed for non-essential amino acids that are not substrates of Lat4, for instance proline with about 75% reduction followed by histidine, serine and alanine. Also Lat4 substrates appeared to be reduced in *Slc43a2*$^{-/-}$ mice, methionine strongly (>50%) and branched-chain AAs less, but their decrease was not statistically significant. The only Lat4 substrate, which didn't appear to be decreased was phenylalanine. Thus, in analogy to the previous AA measurements in amniotic fluids, this blood AA pattern does not reflect a specific lack of Lat4 substrates, but results probably from the interplay of transport and metabolic pathways that are altered in the *Slc43a2*$^{-/-}$ mice. Additionally to the decrease in plasma amino acids, an increase of plasma acylcarnitine-conjugated fatty acids, in particular of dicarboxylic acids and long chain unsaturated fatty acids was detected, which also highlights a state of malnutrition (Fig. 6C and D). As regards glucose homeostasis, *Slc43a2*$^{-/-}$ mice sacrificed at day 2 showed a high blood concentration variability compared to *Slc43a2*$^{+/+}$ and *Slc43a2*$^{+/-}$ mice (Fig. 6B). Hypothesizing that this variability was due to different feeding status of single animals and that *Slc43a2*$^{-/-}$ pups might display a defect in glucose disposal (impaired insulin release) and gluconeogenesis, pups were starved 30 min before sacrifice and blood collection (Fig. 6E). Indeed, in these conditions all *Slc43a2*$^{-/-}$ mice displayed a reduction in blood glucose concentration of about 50% compared to their wild type littermates. Heterozygous *Slc43a2*$^{+/-}$ mice showed in this and also in all other tested parameters no difference with their *Slc43a2*$^{+/+}$ littermates.

Since *Slc43a2*$^{-/-}$ pups displayed a failure to grow and signs of malnutrition, we made attempts to rescue them. Considering that an early defect in weight gain might represent a competitive disadvantage for obtaining breastfeeding within a large litter, we decreased this potential disadvantage by removing all *Slc43a2*$^{+/-}$ littermates on day 3, leaving only an equal number of

Slc43a2$^{+/+}$ and *Slc43a2*$^{-/-}$ pups (Supplementary Figure 2). However, also in the context of reduced litters, *Slc43a2*$^{-/-}$ mice did not grow and/or survive better. Another attempt to compensate malnutrition by subcutaneous administration of an AA-containing solution (Aminoven 10%, Fresenius KABI, 80 µl injection twice a day) did also not increase the weight gain and/or the lifespan of *Slc43a2*$^{-/-}$ mice.

Liver morphology and gene expression of *Slc43a2* null pups

Since the liver plays a central role in nutrients metabolism, we investigated the possible impact of *Slc43a2* defect on its morphology and gene expression pattern. Histological staining showed indeed sites of leucocyte infiltration in its periportal regions (Fig. 7B). Liver RNA-sequencing identified 16'078 transcripts as 'present' (Tophat software) with 1433 displaying a statistically significant ($p < 0.01$) differential expression (Fig. 7A). From these transcripts, the expression of 144 was changed more than three-fold, 77 up- and 67 downwards (Supplementary Table 1). Among the upregulated genes, many are known to be involved in liver regeneration (*Dmbt1* (Bisgaard *et al.*, 2002)), cell proliferation (*Htr2b* (Soll *et al.*, 2010)), tissue remodeling (*Mep1a* and *Mep1b* (Sterchi *et al.*, 2008)) and detoxification (*Gpx6 and Ggt6* (Gridley *et al.*, 2011) (Heisterkamp *et al.*, 2008)). Interestingly, the transcripts encoding acetyl-CoA carboxylase β (*Acab*), involved in lipogenesis (Postic & Girard, 2008) and glucokinase (*Gck*), involved in liver gluconeogenesis (Massa *et al. 2011*), were also upregulated. In contrast, genes involved in fatty acids biosynthesis like *Fas, Srbp1* and *Scd1* were not significantly changed. As expected based on the leucocyte infiltration, *Cyp2a5* and *Ceacam3* expression was increased (Sipowicz *et al.*, 1997). The downregulation of the transcripts *Car3, Dio3* and *Inmt* as well as of genes involved in hepatobiliary cholesterol excretion (*Abcg5* and *Abcg8* (Back *et al.*, 2013)) and circadian clock (*Dbp* (Ando *et al.*, 2011)) similarly suggest major metabolic changes, inflammation, toxicity and regeneration at the level of the liver (Hsieh *et al.*, 2009; Dudek *et al.*, 2013) that might explain in part the increase in plasma fatty acids and the selective decrease of plasma AAs.

At the level of the kidney that also plays an important role for the systemic metabolism of amino acids (Makrides *et al*., 2014 Comp Physiol), we tested the expression of AA transporters, but did not identify any major alterations in *Slc43a2*$^{-/-}$ mice (Fig. 7C). Interestingly, other AA transporters of the SLC43 family, i.e. Lat3 and Eeg1, did not show any differential expression in *Slc43a2*$^{-/-}$ mice; therefore, the lack of Lat4 is not leading to any compensatory regulation of amino acids transporters with similar substrate affinities.

Accumulation of leucine in the proximal part of the small intestine

The major metabolic changes described above suggested that the early death of *Slc43a2*$^{-/-}$ mice might be due to a status of malnutrition. Since we showed that Lat4 is expressed at the basolateral membrane of enterocytes (Fig. 2), we hypothesized that this malnutrition might result from a defective intestinal AA absorption. To test this hypothesis, we starved pups for 30 min and then fed them with 5 µl of an AA solution containing 1 mM of each leucine and lysine with corresponding ^{3}H and ^{14}C tracers. Leucine was chosen as Lat4 substrate because it is not transported by the other basolateral uniporter Tat1, whereas lysine was chosen because it is not transported by Lat4. Upon administration of this AA mixture, we monitored the appearance of the labeled AAs in plasma and their accumulation in different organs after 30 min (Fig. 88). Compared to wild type littermates, pups lacking Lat4 displayed a marked 2-fold increased retention of leucine, but not of lysine, in the first part of the small intestine (Fig. 8A and C). This selective retention of the Lat4 substrate leucine in the small intestine of *Slc43a2*$^{-/-}$ pups suggests its intracellular retention in the absence of basolateral Lat4. This selective retention was not associated with a visible morphological difference as observed on hematoxylin and eosin stained small intestine sections. It also didn't lead to differences in terms of AA appearance in plasma or levels in other organs after 30 min (Fig. 8B and 8D).

Discussion

Lat4 is considered a 'system L' transporter because it transports large neutral AAs independent of Na^+. This functional denomination however does not include other important transport characteristics like transport type and affinity that clearly differentiate Lat4 from the classical system L transporters Lat1 and Lat2 (Lat1-4F2hc/*Slc7a5-Slc3a2* and Lat2-4F2hc/*Slc7a8-Slc3a2*). Indeed, as originally suggested by Bodoy *et al.* (Bodoy *et al.*, 2005), Lat4 functions as a uniporter (facilitated diffusion pathway) and we show here that it does this with a low, symmetrical apparent affinity (Fig. 3). These functional characteristics contrast with those of the classical system L transporters Lat1 and Lat2 that function as asymmetric antiporters with high apparent affinity for the uptake of their substrates (Meier *et al*., 2002). Additionally, the selectivity of Lat4 is more limited and includes only essential AAs, specifically the branched-chain ones plus phenylalanine and methionine. Since the *in vivo* role of this AA transporter has yet not been investigated, we here further analyzed its localization and tested its physiological function using a newly generated general KO mouse model.

The main observation reported here is the fact that mice defective in Lat4 suffer from a small intrauterine growth restriction, a major postnatal growth defect and premature death within a few days after birth, despite normal feeding behavior suggested by the “milk spot”. The question is thus what functional defect the lack of Lat4 provokes, which leads to this developmental problem. The phenotype does not appear to depend on the genetic background since it was not modified by backcrossing for 6 generations with C57BL/6 or S129 mice. Despite the fact that attempts to rescue the pups by litter size reduction (decreased competition) or parenteral nutritional supplementation didn't succeed, we consider it likely that this lethal phenotype is largely due to a combination of defective placental and in particular intestinal AA transport that leads to severe postnatal malnutrition.

Lat4 is a basolateral uniporter for essential neutral AAs in small intestine and kidney tubule

A first crucial aspect towards understanding the function of Lat4 is its tissue and subcellular localization. In the original study of Bodoy *et al.*, which reported its identification and mRNA expression in human and mouse tissues, Lat4 mRNA was shown to be present at high levels in placenta, kidney and small intestine as well as at lower levels in several other tissues and in a proximal tubule cell line (Bodoy *et al*., 2005). Additionally, expression data from microarray analysis available on internet (Biogps.com) indicate a strong expression also in macrophages, microglia and osteoclasts. As previously hypothesized by us, we show here using a newly generated antibody that Lat4 localizes to the basolateral membrane of AA transporting cells of small intestine

and kidney proximal tubule and confirm the selectivity of the staining at these locations using the KO mouse model. These images show that Lat4 is expressed in the small intestine at a much higher level in the villi than in the crypts, similar to other AA transporters involved in transepithelial transport (Fig. 2A,B) (Dave *et al.*, 2004). These data strongly support the hypothesis that Lat4 plays an important role for the (re)absorption of AAs. Interestingly in kidney, next to a strong labeling in the proximal tubule (Fig. 2C-E), there is also a strong basolateral labeling in the thick ascending limb of Henle's loop and a weaker signal in the distal convoluted tubule (Fig. 2F-H). The low level or absence of Lat4 protein expression in liver and skeletal muscle suggested by previous mRNA data is also confirmed by our immunofluorescence results (Fig. 1E-H).

As demonstrated in this study with expression experiments in *Xenopus laevis* oocytes, Lat4 is a symmetrical uniporter with low affinity for its substrates (Fig. 3). Thus, at physiological substrate concentrations, its directional transport activity is proportional to the transmembrane substrate concentration difference. This allows Lat4, if expressed at a sufficiently high level, to mediate the equilibration of its AA substrates (branched chain AAs, phenylalanine and methionine) between the extracellular space and the cytosol. It can thus mediate a directional transport of its substrates across the plasma membrane, for instance their basolateral efflux from small intestine and kidney proximal tubule cells following their luminal uptake from the intestinal lumen or primary urine. We postulate that this directional basolateral efflux transport represents also a recycling pathway for AAs that are taken up across the same basolateral membranes with high affinity by the parallel localized heterodimeric antiporters *Slc7a8-Slc3a2*/Lat2-4F2hc and *Slc7a7-Slc3a2*/y^+Lat1-4F2hc. Such a high affinity uptake of essential AAs by these antiporters allows them to efflux in exchange non-essential AAs present mostly at much higher concentration than essential amino acids in these epithelial cells. Thus, Lat4 may exert a quantitative control of the Lat2 and y^+Lat1 antiporter efflux activity by recycling to the outside the essential AAs they take up in exchange. Correspondingly, the expectation is that the lack of Lat4 could affect the transepithelial transport of other, in particular non-essential and cationic AAs. Such a functional relationship/cooperation with antiporters for the efflux of non-essential AAs has previously been demonstrated in the *Xenopus laevis* oocytes expression system and *in vivo* for the aromatic AA transporter Tat1, another essential AA uniporter expressed at the basolateral membrane of transporting epithelial cells (Ramadan *et al.*, 2007; Mariotta *et al.*, 2012). However, in the present case functional experiments aiming at testing the impact of Lat4 defect on the transport of AAs were strongly limited by the fact that Lat4 mice did not develop normally and died a few days after birth.

As regards Lat4 localization, an intriguing observation is that Lat4 is expressed at a high level also in kidney thick ascending limb, as previously shown at the mRNA level (Cheval *et al.*, 2011). We

postulate that the basolateral expression of Lat4 in these cells plays a role rather for energy metabolism and/or for the synthesis of the highly abundant secreted surface protein uromodulin (Glaudemans *et al*. 2014) than for the transepithelial transport of AAs. These cells might thus import branched-chain AAs and methionine via Lat4 to use them for protein synthesis and as catabolic substrates for the production of ATP or to drive the influx of non-essential AAs, such as glutamine, that then function as metabolic fuel (opposite net transport direction compared to transepithelial transport).

Prenatal and postnatal failure to grow, malnutrition and death of *Slc43a2*$^{-/-}$ knockout mice

The global disruption of the AA uniporter Lat4 highlighted the pivotal importance of this AA transporter in the prenatal and postnatal development. *Slc43a2*$^{-/-}$ KO mice displayed namely defective growth before birth with about a ~10% reduction of weight at embryonic day 18 compared to wildtype littermates. The reported defective growth showed phenotypical analogies with other KO mouse models of AA transporters like y^+Lat1 and CAT-1 (Sperandeo *et al.* 2007;, Xie *et al.* 2005), suggesting that Lat4 should be also considered together with the aforementioned AA transporters as a very important player in placental AA transport. Interestingly, Lat4 dysfunction resulted not only in reduction of its AA substrates in the amniotic fluid, but rather to a general decrease of all AAs with the only exception of aspartate and glutamate. Thus, defective Lat4 function causes pleiotropic consequences that are not limited to a lack of Lat4-specific substrates but encompass many other amino acids. The reduced weight and reduced concentration of AAs in the amniotic fluid did not result in prenatal lethality and did not disrupt the postnatal feeding behavior as suggested by the presence of a normal “milk spot”. However, as shown by the postnatal growth curve and the concentration of different metabolites in plasma of 3 days old mice, it appears that they display a defect in enteric AA absorption that could be the origin of the postnatal growth defect and could contribute to a major extent to the premature lethality of *Slc43a2*$^{-/-}$ mice.

Indeed, the metabolic status of the *Slc43a2*$^{-/-}$ pups already 3 days after birth shows many analogies with starvation. At first glance, surprisingly methionine is the only Lat4 substrate to be highly decreased in their plasma, whereas branched-chain AAs and phenylalanine show only a minor reduction. In contrast, many non-essential amino acids are markedly decreased, mostly alanine and proline. However, based on the suggested function of Lat4 as a 'gate keeper' for the epithelial basolateral efflux of non-essential AAs via antiporters (see above), it is not surprising that a *Slc43a2*$^{-/-}$induced defect in AA absorption may lead to a catabolic state in which the decrease in non-essential AAs is more marked than that of essential ones (Fig. 9).

Interestingly, non-essential AAs are also specifically decreased in fasted children (Wolfsdorf *et al.*, 1982) and upon prolonged endurance exercise, in particular alanine and proline that are central for AA metabolism and gluconeogenesis (Ji *et al.*, 1987; Huq *et al.*, 1993). Also the decrease in tyrosine, histidine and serine can be explained by their catabolic usage to provide substrates for the Krebs cycle. The increase in plasma acylcarnitine-conjugated dicarboxylic and long-chain unsaturated fatty acids in *Slc43a2*$^{-/-}$ mice is an additional metabolic fingerprint indicating that the *Slc43a2*$^{-/-}$ pups are in a state of starvation (Costa *et al.*, 1999; Hunt & Alexson, 2002). Additionally, the histological examination and the gene expression analysis of the liver, by indicating processes of inflammation, regeneration and alteration of glucose and fatty acids metabolism, further indicated that *Slc43a2* null pups suffered from malnutrition. Indeed, an alteration in glucose metabolism, which is a hallmark of nutritional defects in children (Bandsma *et al.*, 2010; Spoelstra *et al.*, 2012) was also present in *Slc43a2*$^{-/-}$ mice as shown by the marked decrease in blood glucose concentration measured upon 30 min starvation.

The hypothesis that Lat4 impacts on AA absorption was further supported by our observation that leucine administered orally was retained in the proximal part of the small intestine of *Slc43a2*$^{-/-}$ mice unlike lysine which is not a Lat4 substrate. This suggests that leucine, taken up luminally, accumulated in small intestine enterocytes from which it could not be efficiently released basolaterally. However, we didn't observe in these mice a concomitant alteration in plasma appearance or organ accumulation of leucine such that this experiment did not verify a possible major defect in AA absorption from ingested food. It is however possible that the non-physiological administration of two AAs at a high concentration (1 mM each) to a large extent bypassed a defect preventing sufficient absorption from mother's milk. An additional possibility that could not be tested is that the amino acids permanently secreted by the liver and the pancreas into the intestine lumen as well as the amino acids resulting from enterocyte shedding were not efficiently reabsorbed, leading finally to a substantial amino acids loss into the feces.

An interesting observation is that out of five KO mouse models lacking amino acid transporters expressed in small intestine and kidney proximal tubule, the KO of Lat4 is only the second one that leads to a lethal phenotype. Neither the lack of luminal B^0AT1 transporter, nor the lack of the basolateral L-type antiporter Lat2 (*Slc7a8*) and of the aromatic amino acid uniporter Tat1 (*Slc16a10*) prevent normal life and reproduction in laboratory conditions. The KO of Lat4 is the first AA transporter defect that despite a normal Mendelian birth ratio leads to a severe postnatal malnutrition with early death. Many observations presented here suggest that the primary cause of *Slc43a2*$^{-/-}$ pups malnutrition may be a defect in AA absorption from the gut. However, it was not formally excluded that the observed malnutrition syndrome was in part due to an insufficient

suckling drive or another alteration preventing the appropriate use of mother's milk as nutrition source.

In addition to the aforementioned points, we considered the possibility that Lat4 deficiency, because of its high expression in macrophages and microglia (BioGPS.org), could impact on the survival of the pups by affecting the immune system. However, transgenic mice with defective hematopoietic mononuclear phagocytic cells, e.g. Csfr1$^{-/-}$ KO (Dai *et al*. 2002) or op/op mice (Wiktor-Jedrzejczak *et al*. 1990) have been shown to survive beyond weaning, clearly indicating that the lethality of Lat4 KO mice is not due to an immune defect.

In conclusion, we provided here the first characterization of a total *Slc43a2* KO mouse model. The small intrauterine growth retardation and the postnatal malnutrition phenotype leading to an early death indicate that Lat4 is an essential AA transporter required for the proper placental AA transport and postnatal nutrient absorption.

References

Ando H, Kumazaki M, Motosugi Y, Ushijima K, Maekawa T, Ishikawa E & Fujimura A (2011). Impairment of peripheral circadian clocks precedes metabolic abnormalities in ob/ob mice. *Endocrinology* **152,** 1347-1354.

Babu E, Kanai Y, Chairoungdua A, Kim DK, Iribe Y, Tangtrongsup S, Jutabha P, Li Y, Ahmed N, Sakamoto S, Anzai N, Nagamori S & Endou H (2003). Identification of a novel system L amino acid transporter structurally distinct from heterodimeric amino acid transporters. *J Biol Chem* **278,** 43838-43845.

Back SS, Kim J, Choi D, Lee ES, Choi SY & Han K (2013). Cooperative transcriptional activation of ATP-binding cassette sterol transporters ABCG5 and ABCG8 genes by nuclear receptors including Liver-X-Receptor. *BMB Rep* **46,** 322-327.

Bandsma RH, Mendel M, Spoelstra MN, Reijngoud DJ, Boer T, Stellaard F, Brabin B, Schellekens R, Senga E & Heikens GT (2010). Mechanisms behind decreased endogenous glucose production in malnourished children. *Pediatr Res* **68,** 423-428.

Bisgaard HC, Holmskov U, Santoni-Rugiu E, Nagy P, Nielsen O, Ott P, Hage E, Dalhoff K, Rasmussen LJ & Tygstrup N (2002). Heterogeneity of ductular reactions in adult rat and human liver revealed by novel expression of deleted in malignant brain tumor 1. *Am J Pathol* **161,** 1187-1198.

Bodoy S, Martin L, Zorzano A, Palacin M, Estevez R & Bertran J (2005). Identification of LAT4, a novel amino acid transporter with system L activity. *J Biol Chem* **280,** 12002-12011.

Borsani G, Bassi MT, Sperandeo MP, De Grandi A, Buoninconti A, Riboni M, Manzoni M, Incerti B, Pepe A, Andria G, Ballabio A & Sebastio G (1999). SLC7A7, encoding a putative permease-related protein, is mutated in patients with lysinuric protein intolerance. *Nat Genet* **21,** 297-301.

Braun D, Wirth EK, Wohlgemuth F, Reix N, Klein MO, Gruters A, Kohrle J & Schweizer U (2011). Aminoaciduria, but normal thyroid hormone levels and signaling, in mice lacking the amino acid and thyroid hormone transporter Slc7a8. *Biochem J* **439,** 249-255.

Broer S & Palacin M (2011). The role of amino acid transporters in inherited and acquired diseases. *Biochem J* **436,** 193-211.

Camargo SM, Singer D, Makrides V, Huggel K, Pos KM, Wagner CA, Kuba K, Danilczyk U, Skovby F, Kleta R, Penninger JM & Verrey F. (2009). Tissue-specific amino acid transporter partners ACE2 and collectrin differentially interact with hartnup mutations. *Gastroenterology* **136,** 872-882.

Cheval L, Pierrat F, Dossat C, Genete M, Imbert-Teboul M, Duong Van Huyen JP, Poulain J, Wincker P, Weissenbach J, Piquemal D & Doucet A (2011). Atlas of gene expression in the mouse kidney: new features of glomerular parietal cells. *Physiol Genomics* **43,** 161-173.

Cleal JK, Glazier JD, Ntani G, Crozier SR, Day PE, Harvey NC, Robinson SM, Cooper C, Godfrey KM, Hanson MA & Lewis RM. (2011). Facilitated transporters mediate net efflux of amino acids to the fetus across the basal membrane of the placental syncytiotrophoblast. *J Physiol* **589,** 987-997.

Costa CC, de Almeida IT, Jakobs C, Poll-The BT & Duran M (1999). Dynamic changes of plasma acylcarnitine levels induced by fasting and sunflower oil challenge test in children. *Pediatr Res* **46**, 440-444.

Dai XM, Ryan GR, Hapel AJ, Dominguez MG, Russell RG, Kapp S, Sylvestre V & Stanley ER. (2002). Targeted disruption of the mouse colony-stimulating factor 1 receptor gene results in osteopetrosis, mononuclear phagocyte deficiency, increased primitive progenitor cell frequencies, and reproductive defects. *Blood* **99,** 111-120.

Danilczyk U, Sarao R, Remy C, Benabbas C, Stange G, Richter A, Arya S, Pospisilik JA, Singer D, Camargo SM, Makrides V, Ramadan T, Verrey F, Wagner CA & Penninger JM (2006). Essential role for collectrin in renal amino acid transport. *Nature* **444,** 1088-1091.

Dave MH, Schulz N, Zecevic M, Wagner CA & Verrey F (2004). Expression of heteromeric amino acid transporters along the murine intestine. *J Physiol* **558,** 597-610.

Dudek KM, Suter L, Darras VM, Marczylo EL & Gant TW (2013). Decreased translation of Dio3 mRNA is associated with drug-induced hepatotoxicity. *Biochem J* **453,** 71-82.

Dumont JN (1972). Oogenesis in Xenopus laevis (Daudin). I. Stages of oocyte development in laboratory maintained animals. *J Morphol* **136,** 153-179.

Fickert P, Zollner G, Fuchsbichler A, Stumptner C, Pojer C, Zenz R, Lammert F, Stieger B, Meier PJ, Zatloukal K, Denk H & Trauner M (2001). Effects of ursodeoxycholic and cholic acid feeding on hepatocellular transporter expression in mouse liver. *Gastroenterology* **121,** 170-183.

Fukuhara D, Kanai Y, Chairoungdua A, Babu E, Bessho F, Kawano T, Akimoto Y, Endou H & Yan K (2007). Protein characterization of NA+-independent system L amino acid transporter 3 in mice: a potential role in supply of branched-chain amino acids under nutrient starvation. *Am J Pathol* **170,** 888-898.

Glaudemans B, Terryn S, Gölz N, Brunati M, Cattaneo A, Bachi A, Al-Qusairi L, Ziegler U, Staub O, Rampoldi L & Devuyst O (2014). A primary culture system of mouse thick ascending limb cells with preserved function and uromodulin processing. *Pflugers Arch* **466**, 343-56.

Gridley DS, Freeman TL, Makinde AY, Wroe AJ, Luo-Owen X, Tian J, Mao XW, Rightnar S, Kennedy AR, Slater JM & Pecaut MJ (2011). Comparison of proton and electron radiation effects on biological responses in liver, spleen and blood. *Int J Radiat Biol* **87,** 1173-1181.

Heisterkamp N, Groffen J, Warburton D & Sneddon TP (2008). The human gamma-glutamyltransferase gene family. *Hum Genet* **123,** 321-332.

Hsieh HC, Chen YT, Li JM, Chou TY, Chang MF, Huang SC, Tseng TL, Liu CC & Chen SF (2009). Protein profilings in mouse liver regeneration after partial hepatectomy using iTRAQ technology. *J Proteome Res* **8,** 1004-1013.

Hunt MC & Alexson SE (2002). The role Acyl-CoA thioesterases play in mediating intracellular lipid metabolism. *Prog Lipid Res* **41,** 99-130.

Huq F, Thompson M & Ruell P (1993). Changes in serum amino acid concentrations during prolonged endurance running. *Jpn J Physiol* **43,** 797-807.

Ji LL, Miller RH, Nagle FJ, Lardy HA & Stratman FW (1987). Amino acid metabolism during exercise in trained rats: the potential role of carnitine in the metabolic fate of branched-chain amino acids. *Metabolism* **36,** 748-752.

Kaplan MR, Plotkin MD, Lee WS, Xu ZC, Lytton J & Hebert SC (1996). Apical localization of the Na-K-Cl cotransporter, rBSC1, on rat thick ascending limbs. *Kidney Int* **49,** 40-47.

Loffing J, Vallon V, Loffing-Cueni D, Aregger F, Richter K, Pietri L, Bloch-Faure M, Hoenderop JG, Shull GE, Meneton P & Kaissling B (2004). Altered renal distal tubule structure and renal Na(+) and Ca(2+) handling in a mouse model for Gitelman's syndrome. *J Am Soc Nephrol* **15,** 2276-2288.

Makrides V, Camargo SMR, and Verrey F. Transport of amino acids in the kidney (2014). *Comprehensive Physiology* **4,** 367-403.

Mariotta L, Ramadan T, Singer D, Guetg A, Herzog B, Stoeger C, Palacin M, Lahoutte T, Camargo SM & Verrey F (2012). T-type amino acid transporter TAT1 (Slc16a10) is essential for extracellular aromatic amino acid homeostasis control. *J Physiol* **590,** 6413-6424.

Massa ML, Gagliardino JJ & Francini F (2011). Liver glucokinase: An overview on the regulatory mechanisms of its activity. *IUBMB Life* **63,** 1-6.

Meier C, Ristic Z, Klauser S, Verrey F (2002). Activation of system L heterodimeric amino acid exchangers by intracellular substrates. *EMBO J* **21,** 580-589.

Moret C, Dave MH, Schulz N, Jiang JX, Verrey F & Wagner CA (2007). Regulation of renal amino acid transporters during metabolic acidosis. *Am J Physiol Renal Physiol* **292,** F555-566.

Nassl AM, Rubio-Aliaga I, Sailer M & Daniel H (2011). The intestinal peptide transporter PEPT1 is involved in food intake regulation in mice fed a high-protein diet. *PLoS One* **6,** e26407.

Poncet N & Taylor PM (2013). The role of amino acid transporters in nutrition. *Curr Opin Clin Nutr Metab Care* **16,** 57-65.

Postic C & Girard J (2008). Contribution of de novo fatty acid synthesis to hepatic steatosis and insulin resistance: lessons from genetically engineered mice. *J Clin Invest* **118,** 829-838.

Ramadan T, Camargo SM, Herzog B, Bordin M, Pos KM & Verrey F (2007). Recycling of aromatic amino acids via TAT1 allows efflux of neutral amino acids via LAT2-4F2hc exchanger. *Pflugers Arch* **454,** 507-516.

Ramadan T, Camargo SM, Summa V, Hunziker P, Chesnov S, Pos KM & Verrey F (2006). Basolateral aromatic amino acid transporter TAT1 (Slc16a10) functions as an efflux pathway. *J Cell Physiol* **206,** 771-779.

Rudnick G, Krämer R, Blakely RD, Murphy DL & Verrey F (2014). The SLC6 Transporters: perspective on structure, functions, regulation and models for transporter dysfunction (2014). *Pflugers Arch* **466,** 25-42.

Shigeoka T, Kawaichi M & Ishida Y (2005). Suppression of nonsense-mediated mRNA decay permits unbiased gene trapping in mouse embryonic stem cells. *Nucleic Acids Res* **33,** e20.

Sipowicz MA, Chomarat P, Diwan BA, Anver MA, Awasthi YC, Ward JM, Rice JM, Kasprzak KS, Wild CP & Anderson LM (1997). Increased oxidative DNA damage and hepatocyte overexpression of specific cytochrome P450 isoforms in hepatitis of mice infected with Helicobacter hepaticus. *Am J Pathol* **151,** 933-941.

Soll C, Jang JH, Riener MO, Moritz W, Wild PJ, Graf R & Clavien PA (2010). Serotonin promotes tumor growth in human hepatocellular cancer. *Hepatology* **51,** 1244-1254.

Sperandeo MP, Annunziata P, Bozzato A, Piccolo P, Maiuri L, D'Armiento M, Ballabio A, Corso G, Andria G, Borsani G & Sebastio G (2007). Slc7a7 disruption causes fetal growth retardation by downregulating Igf1 in the mouse model of lysinuric protein intolerance. *Am J Physiol Cell Physiol* **293,** C191-198.

Spoelstra MN, Mari A, Mendel M, Senga E, van Rheenen P, van Dijk TH, Reijngoud DJ, Zegers RG, Heikens GT & Bandsma RH (2012). Kwashiorkor and marasmus are both associated with impaired glucose clearance related to pancreatic beta-cell dysfunction. *Metabolism* **61,** 1224-1230.

Sterchi EE, Stocker W & Bond JS (2008). Meprins, membrane-bound and secreted astacin metalloproteinases. *Mol Aspects Med* **29,** 309-328.

Taylor MA & Smith LD (1987). Accumulation of free amino acids in growing Xenopus laevis oocytes. *Dev Biol* **124,** 287-290.

Verrey F, Singer D, Ramadan T, Vuille-dit-Bille RN, Mariotta L & Camargo SM (2009). Kidney amino acid transport. *Pflugers Arch* **458,** 53-60.

Wagner CA, Loffing-Cueni D, Yan Q, Schulz N, Fakitsas P, Carrel M, Wang T, Verrey F, Geibel JP, Giebisch G, Hebert SC & Loffing J (2008). Mouse model of type II Bartter's syndrome. II. Altered expression of renal sodium- and water-transporting proteins. *Am J Physiol Renal Physiol* **294,** F1373-1380.

Wiktor-Jedrzejczak W, Bartocci A, Ferrante AW, Jr., Ahmed-Ansari A, Sell KW, Pollard JW & Stanley ER. (1990). Total absence of colony-stimulating factor 1 in the macrophage-deficient osteopetrotic (op/op) mouse. *Proc Natl Acad Sci U S A* **87,** 4828-4832.

Wolfsdorf JI, Sadeghi-Nejad A & Senior B (1982). Hypoalaninemia and ketotic hypoglycemia: cause or consequence? *Eur J Pediatr* **138,** 28-31.

Wu G (2009). Amino acids: metabolism, functions, and nutrition. *Amino Acids* **37,** 1-17.

Xie X, Dumas T, Tang L, Brennan T, Reeder T, Thomas W, Klein RD, Flores J, O'Hara BF, Heller HC & Franken P. (2005). Lack of the alanine-serine-cysteine transporter 1 causes tremors, seizures, and early postnatal death in mice. *Brain Res* **1052,** 212-221.

Competing interests: All authors declare no competing financial, personal, or professional interests that could be construed to have influenced this paper.

Author contributions: Conception and design of the experiment: A.G., L.M. and F.V. Collection, analysis and interpretation of data: A.G., L.M., L.B., B.H., R.F., S.M.R.C. and F.V. Drafting and revising the article: A.G. and F.V. All authors approved the final version.

Funding: The laboratory of FV is supported by Swiss NSF grant 31-130471/1 and the National Centre of Competence in Research (NCCR) Kidney.CH.

Acknowledgments: The authors thank Giancarlo Russo for his help with the analysis of the RNA sequencing data and Achim Weber for his help with the liver histological analysis.

Figure legends:

Figure 1. Confirmation of Lat4 deletion and validation of Lat4 antibody by immunofluorescence on tissue of wild type and Lat4 knock-out pups. A basolateral signal is seen with Lat4 antibody (*green*) in kidney (**A**) and small intestine (**C**) of 3 days old wildtype pups; whereas no such signal is visible ono sections from knock-out littermates (**B** and **D**). No signal (*green*) is observed in skeletal muscle (**E**) and liver (**G**) of wildtype pups besides background also visible in the knock-outs (**F** and **H**). As luminal marker for kidney proximal tubule cells, Tmem27 (*red*) was used (**A** and **B)** and for the canalicular membrane of liver hepatocytes, MDR1 was used (*red*) (**G** and **H)**. Scale bars: 20 μm.

Figure 2. Localization of Lat4 on small intestine and kidney sections by immunofluorescence. (**A** and **B**) On these duodenum sections a strong Lat4 signal (*green*) is visible at the basolateral membrane of enterocytes all along the villi (V) but not in the crypts (C). DAPI (*blue*) was used to label the nuclei. (**C**) Lat4 (*green*) is expressed at the basolateral side of kidney proximal tubule (PT) cells identified by luminal protein Tmem27 (*red*) and by the basolateral co-localization (arrows) with the aromatic AA uniporter Tat1 (*pink*) visible on a consecutive section (**D** and **E**). (**F**) Labeling with NCC (luminal, *red*) identifies the distal convoluted tubule where a weaker expression of Lat4 (*green*) is visible, whereas in thick ascending limb (TAL) identified by the luminal marker NKCC2 (**G** and **H**) a strong signal for Lat4 (green) is visible. Scale bar: 20 μm.

Figure 3. Concentration-dependence of L-phenylalanine uptake and efflux in *X. laevis oocytes* expressing human LAT4. Oocytes were injected with 25 ng of hSLC43A2 cRNA and incubated for 3 days. (**A**) Concentration-dependent uptakes were performed for 10 min with 9 different concentrations of phenylalanine; n = 8-24 oocytes pooled from three independent experiments. (**B**) For the efflux experiments, oocytes were injected with 50 nl of phenylalanine at 5 different concentrations; n = 12-14 oocytes pooled from three independent experiments. Represented are means and SEM. Curves corresponding to the Michaelis-Menten equation were fitted to the experimental data using a non-linear regression routine (Graph Prism 5.0).

Figure 4. Effect of *Slc43a2* deletion on intrauterine growth and amino acids concentration in amniotic fluid at embryonic day 18. (**A**) Representative picture of E18 *Slc43a2*$^{+/+}$ and *Slc43a2*$^{-/-}$ foeti with corresponding weights (**B**) and amino acids concentration in amniotic fluids (**C**). Results were normalized to *Slc43a2*$^{+/+}$ (1.0) and represent means ± SEM of data pooled from two independent experiments, n = 7 for *Slc43a2*$^{+/+}$ mice, n = 15 for *Slc43a2*$^{+/-}$ mice and n = 4 for

Slc43a2$^{-/-}$ mice. Two-way ANOVA, Dunnet's Multiple Comparison posttest for (**B**) and Bonferroni posttest for (**C**), ** $p < 0.01$. ns: non-significant.

Figure 5. Postnatal growth retardation and premature death *of Slc43a2*$^{-/-}$ mice. (**A**) Representative picture of a *Slc43a2*$^{-/-}$ mouse (top) versus a *Slc43a2*$^{+/+}$mouse (bottom) at day 7 after birth. (**B**) Growth curves for *Slc43a2*$^{+/+}$, *Slc43a2*$^{+/-}$ and *Slc43a2*$^{-/-}$ mice; represented are means and SEM, n = 7 for *Slc43a2*$^{+/+}$, n = 22 for *Slc43a2*$^{+/-}$, n = 7 for *Slc43a2*$^{-/-}$; comparison of *Slc43a2*$^{+/+}$ and *Slc43a2*$^{-/-}$ by two-way ANOVA and Bonferroni posttest: ** $p < 0.01$, *** $p < 0.001$; cross represents death of all *Slc43a2*$^{-/-}$ mice. (**C**) Survival curves for the same mice as (**B**).

Figure 6. Impact of *Slc43a2* deletion on plasma amino acids, acylcarnitines and glucose. (**A**) Plasma amino acids, (**C**) long-chain unsaturated acylcarnitines and (**D**) dicarboxylacylcarnitines (DAs). Represented are means and SEM, n = 3 for *Slc43a2*$^{+/+}$ (black bars), n = 6 for *Slc43a2*$^{-/-}$ (white bars), two-way ANOVA, Bonferroni posttest, * $p < 0.05$, ** $p < 0.001$. (**B** and **E**) Blood glucose measurement from mice at day 2 without (**B**) and with 30 min starvation (**E**) prior to sample collection. Represented are means and SEM, Student's *t*-test, ** $p < 0.01$.

Figure 7. Effect of *Slc43a2* deletion on liver and kidney. (**A**) Heatmap summary of differential gene expression pattern in *Slc43a2*$^{-/-}$ liver. RNA was isolated from mice at day 2 and each column represents a different mouse. Upregulated genes are labeled red, downregulated blue. (**B**) Hematoxylin and eosin staining of liver. Left panel: liver section of *Slc43a2*$^{-/-}$ KO mouse. Right panel: liver section of *Slc43a2*$^{+/+}$ mouse. (*) shows leucocyte infiltration in the periportal region of *Slc43a2*$^{-/-}$ mouse liver. Scale bar: 50 μm. (**C**) Gene expression of selected amino acid transporters in the kidney of *Slc43a2*$^{+/+}$ (black bars) and *Slc43a2*$^{-/-}$ (white bars). Represented are means and SEM, n = 3, two-way ANOVA, Bonferroni posttest, ** $p < 0.01$.

Figure 8. Distribution of radiolabeled L-leucine and L-lysine in different organs after oral administration. Mice were starved 30 min prior to oral administration of radiolabeled AA solution. (**A**) leucine and (**C**) lysine accumulation in different organs normalized by weight. (**B**) leucine and (**D**) lysine concentration in plasma 30 min after oral administration (*Slc43a2*$^{+/+}$: black bars, *Slc43a2*$^{-/-}$: white bars). The small intestine of the pups was divided in three equals parts named from proximal to distal: SI1, SI2 and SI3. Represented are means and SEM pooled from three independent experiments, n = 6 for *Slc43a2*$^{+/+}$ mice, n = 8 for *Slc43a2*$^{-/-}$ mice, two-way ANOVA, Bonferroni posttest, *** $p < 0.001$.

Figure 9. Schematic representation of apical and basolateral amino acid transporter cooperation in proximal tubule kidney cell. Neutral amino acids are imported apically mostly via

the symporter B^0AT1 (*SLC6A19*) and are effluxed across the basolateral membrane mostly by the antiporter LAT2-4F2hc and the uniporters TAT1 and LAT4. We postulate that essential neutral amino acids are equilibrated between the intracellular compartment and the extracellular space via the two low affinity uniporters TAT1 and LAT4 and may recycle into the cell via antiporters and thereby drive the efflux of other amino acids, in particular of (non)-essential neutral amino acids via LAT2-4F2hc and cationic amino acids via y^+LAT1-4F2hc. Therefore, a defect in the uniporter(s) LAT4 and/or TAT1 is suggested not only to impact on the basolateral efflux of their own amino acid substrates, but also on that of the other substrates of the antiporters LAT2-4F2hc and y^+LAT1-4F2hc.

Figure 1

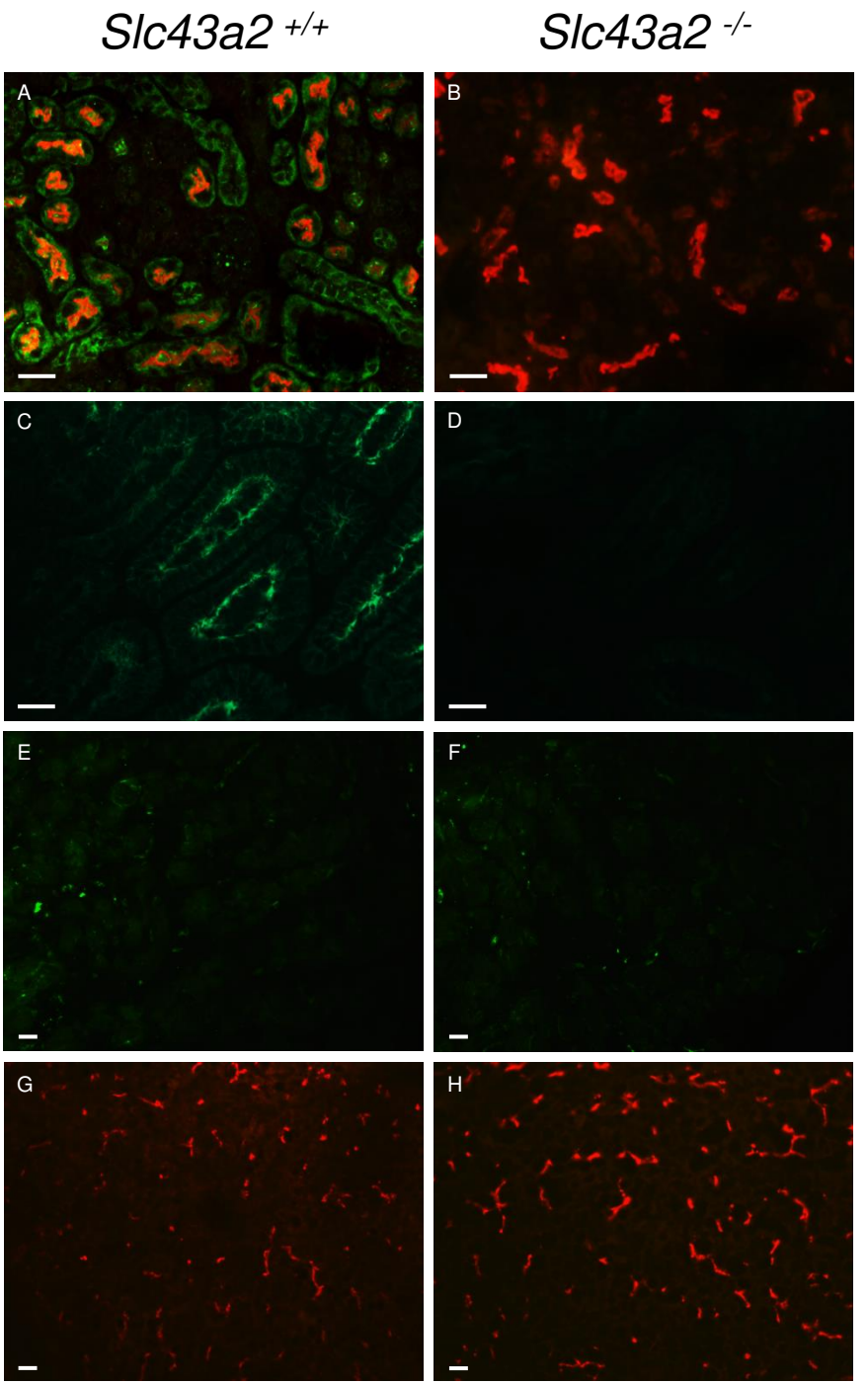

Figure 2

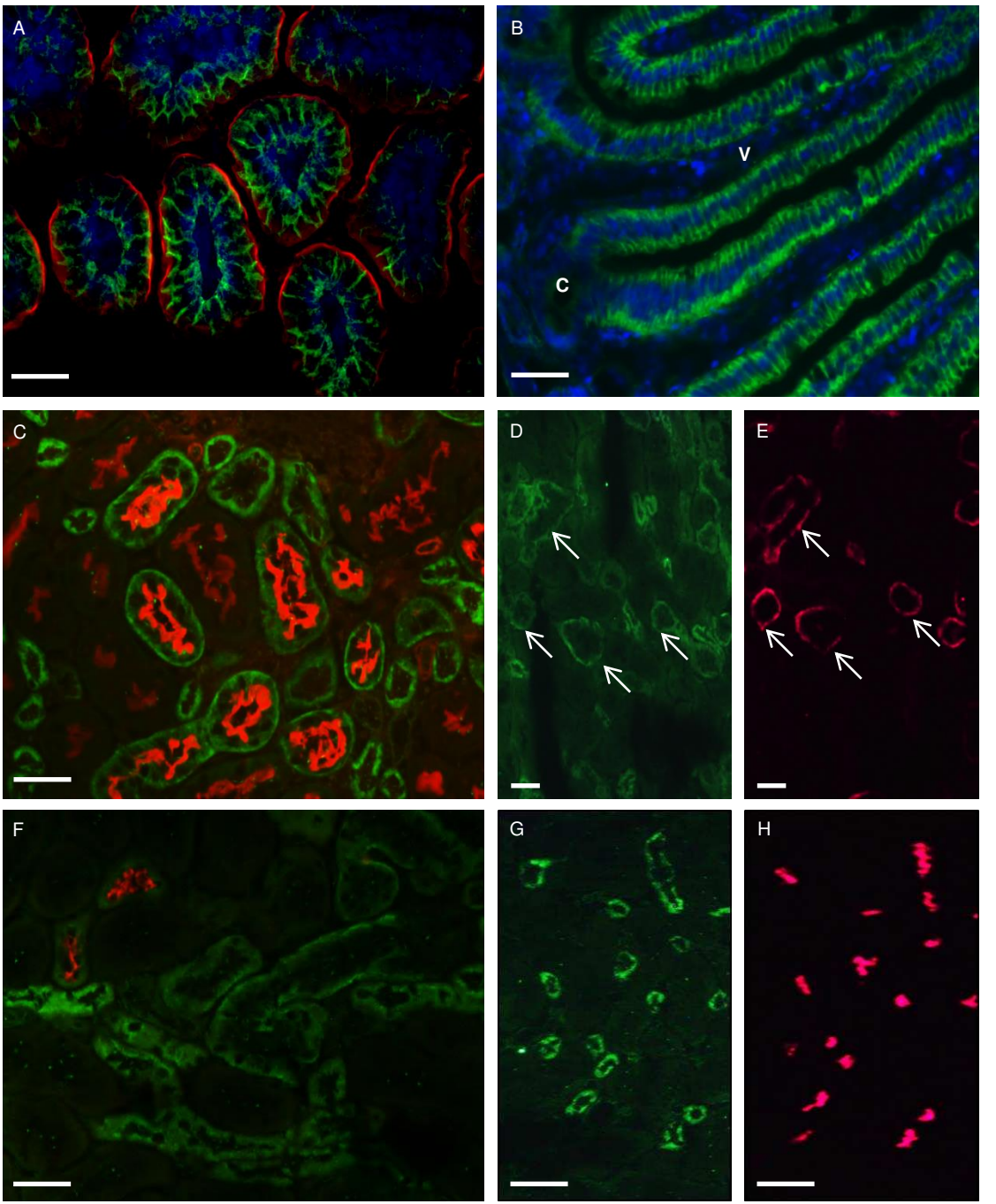

Figure 3

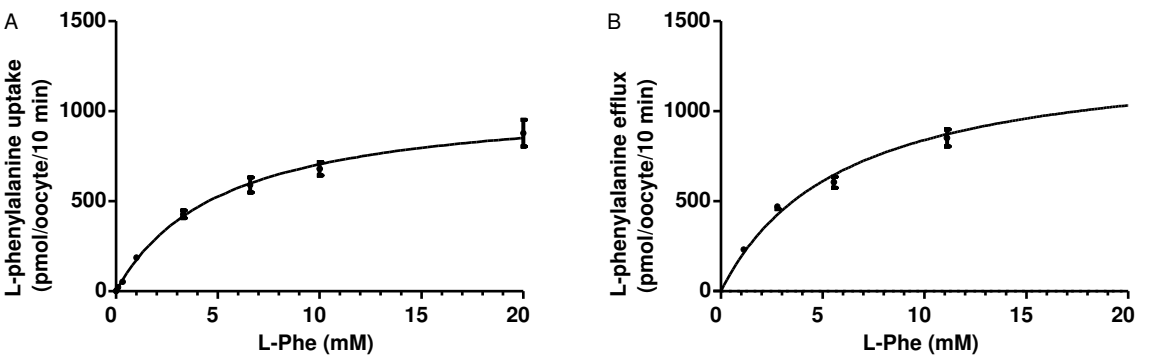
A
1500
1000
500
0
L-phenylalanine uptake
(pmol/oocyte/10 min)
0
5
10
15
20
L-Phe (mM)
B
1500
1000
500
0
L-phenylalanine efflux
(pmol/oocyte/10 min)
0
5
10
15
20
L-Phe (mM)

Figure 4

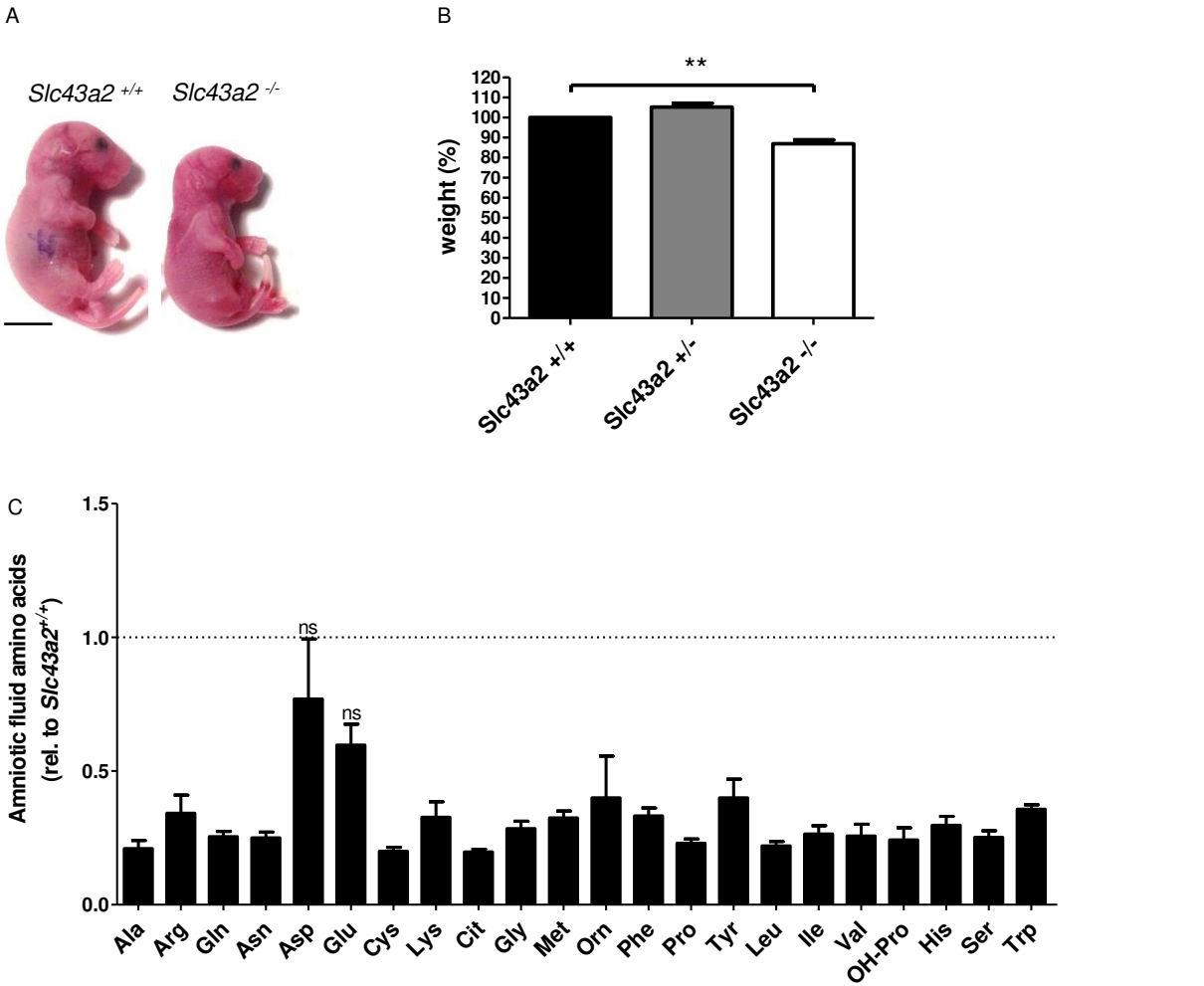
A
Slc43a2 +/+
Slc43a2 -/-
B
**
weight (%)
120
110
100
90
80
70
60
50
40
30
20
10
0
Slc43a2 +/+
Slc43a2 +/-
Slc43a2 -/-
C
Amniotic fluid amino acids
(rel. to Slc43a2+/+)
1.5
1.0
0.5
0.0
ns
ns
Ala
Arg
Gln
Asn
Asp
Glu
Cys
Lys
Cit
Gly
Met
Orn
Phe
Pro
Tyr
Leu
Ile
Val
OH-Pro
His
Ser
Trp

Figure 5

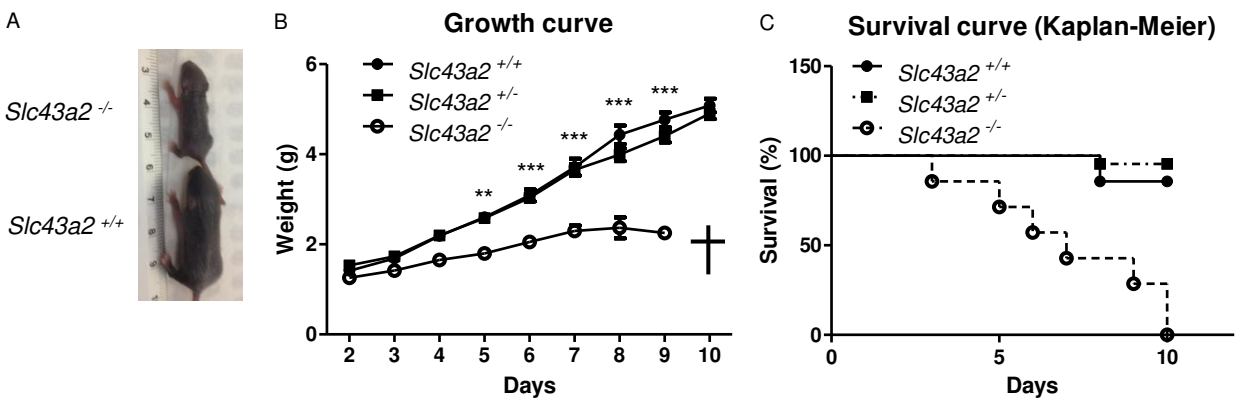
A
Slc43a2 -/-
Slc43a2 +/+
B
Growth curve
Slc43a2 +/+
Slc43a2 +/-
Slc43a2 -/-
Weight (g)
Days
**
***
***
***
***
C
Survival curve (Kaplan-Meier)
Slc43a2 +/+
Slc43a2 +/-
Slc43a2 -/-
Survival (%)
Days

Figure 6

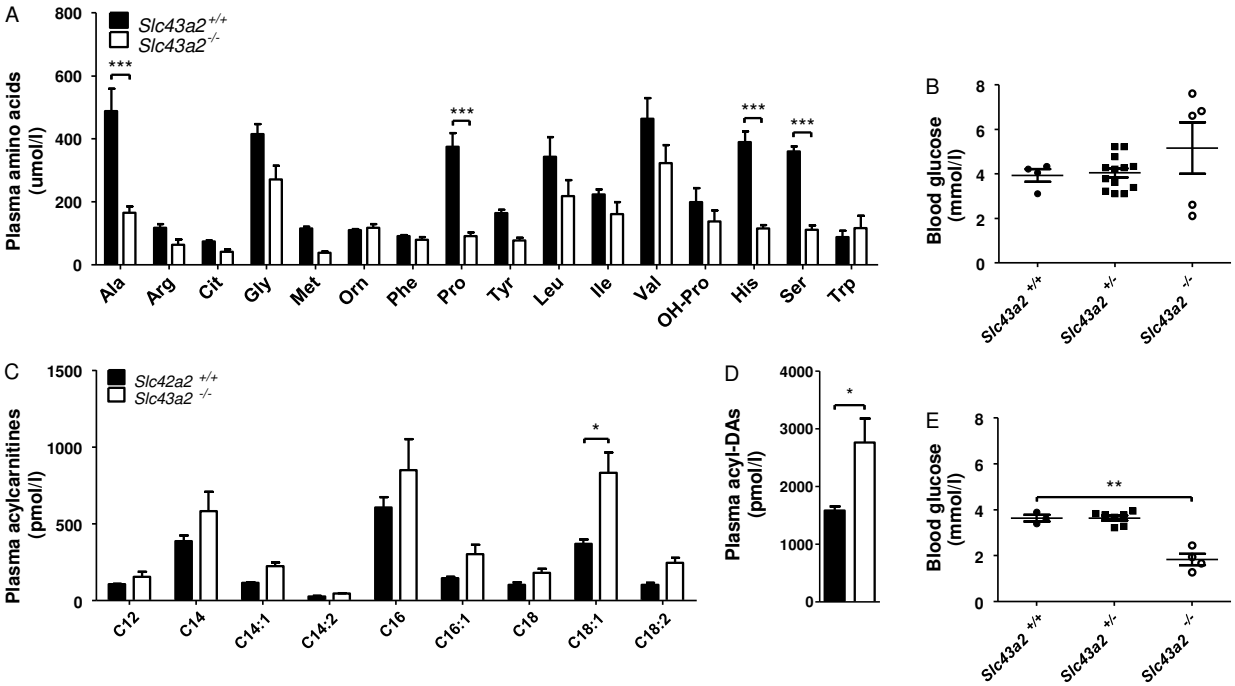
A
Slc43a2 +/+
Slc43a2 -/-
Plasma amino acids (umol/l)
800
600
400
200
0
***
***
***
***
Ala
Arg
Cit
Gly
Met
Orn
Phe
Pro
Tyr
Leu
Ile
Val
OH-Pro
His
Ser
Trp
B
Blood glucose (mmol/l)
8
6
4
2
0
Slc43a2 +/+
Slc43a2 +/-
Slc43a2 -/-
C
Slc42a2 +/+
Slc43a2 -/-
Plasma acylcarnitines (pmol/l)
1500
1000
500
0
*
C12
C14
C14:1
C14:2
C16
C16:1
C18
C18:1
C18:2
D
Plasma acyl-DAs (pmol/l)
4000
3000
2000
1000
0
*
E
Blood glucose (mmol/l)
8
6
4
2
0
**
Slc43a2 +/+
Slc43a2 +/-
Slc43a2 -/-

Figure 7

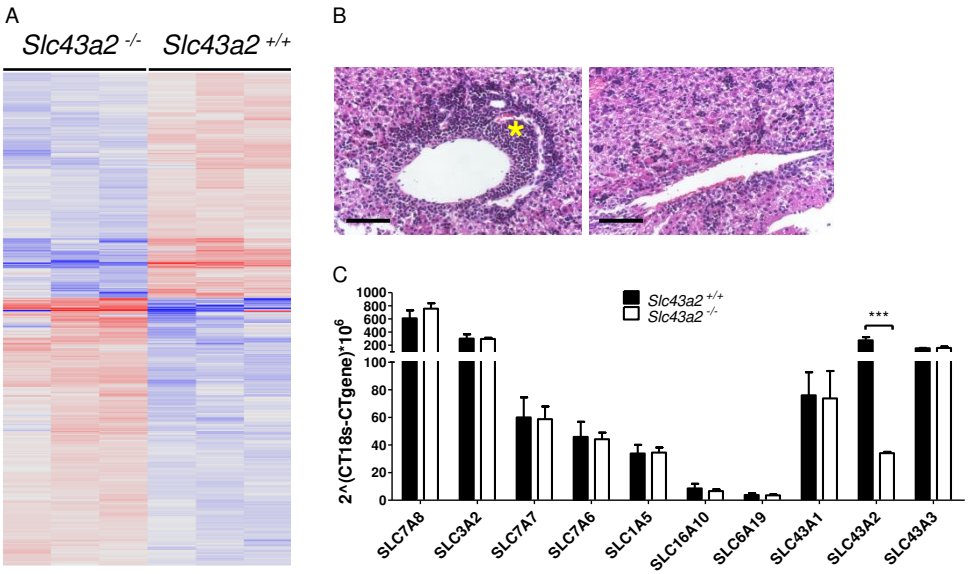
A
Slc43a2 -/-
Slc43a2 +/+
B
C
2^(CT18s-CTgene)*10^6
1000
800
600
400
200
100
80
60
40
20
0
Slc43a2 +/+
Slc43a2 -/-
***
SLC7A8
SLC3A2
SLC7A7
SLC7A6
SLC1A5
SLC16A10
SLC6A19
SLC43A1
SLC43A2
SLC43A3

Figure 8

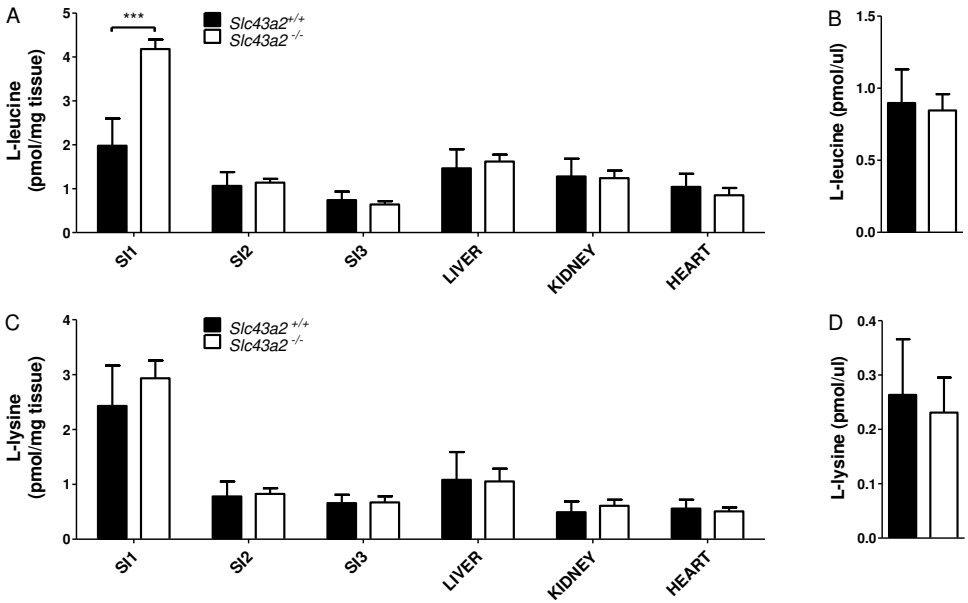
A
***
Slc43a2+/+
Slc43a2-/-
L-leucine (pmol/mg tissue)
0
1
2
3
4
5
SI1
SI2
SI3
LIVER
KIDNEY
HEART
B
L-leucine (pmol/ul)
0.0
0.5
1.0
1.5
C
Slc43a2+/+
Slc43a2-/-
L-lysine (pmol/mg tissue)
0
1
2
3
4
SI1
SI2
SI3
LIVER
KIDNEY
HEART
D
L-lysine (pmol/ul)
0.0
0.1
0.2
0.3
0.4

Figure 9

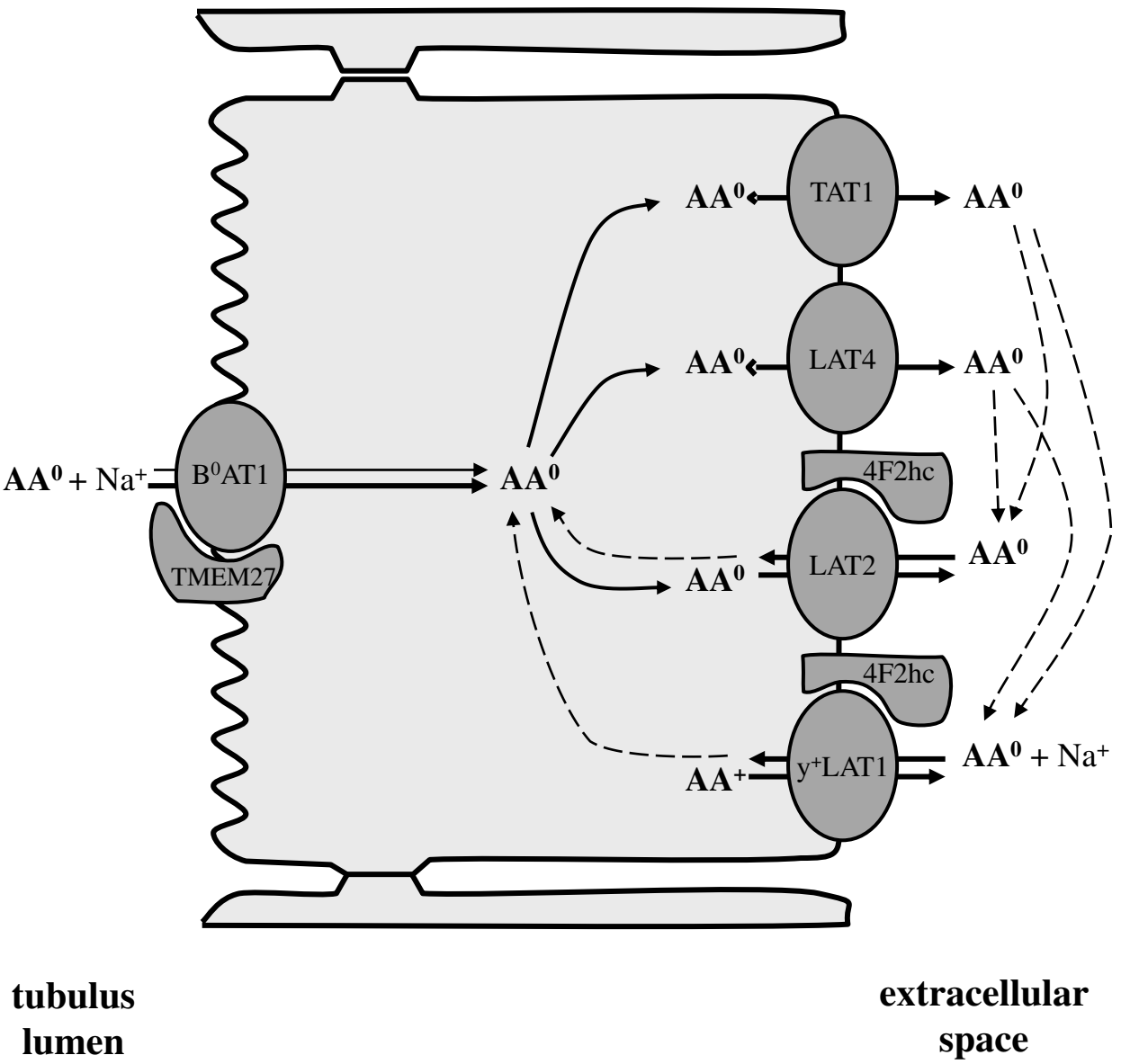
AA⁰
TAT1
AA⁰
AA⁰
LAT4
AA⁰
AA⁰ + Na⁺
B⁰AT1
AA⁰
4F2hc
TMEM27
AA⁰
LAT2
AA⁰
4F2hc
AA⁺
y⁺LAT1
AA⁰ + Na⁺
tubulus lumen
extracellular space